Mesoscopic shelving readout of superconducting qubits in circuit quantum electrodynamics

B. G. U. Englert,[1,2,3,*] G. Mangano,[4,5] M. Mariantoni,[1,3,†] R. Gross,[1,3] J. Siewert,[5,6,7] and E. Solano[6,7]
[1]*Walther-Meißner-Institut, Bayerische Akademie der Wissenschaften, Walther-Meißner-Str. 8, D-85748 Garching, Germany*
[2]*Physik Department, ASC and CeNS, Ludwig-Maximilians-Universität, Theresienstr. 37, D-80333 München, Germany*
[3]*Physik Department, Technische Universität München, D-85748 Garching, Germany*
[4]*MATIS-INFM and Dipartimento di Metodologie Fisiche e Chimiche (DMFCI), viale A. Doria 6, 95125 Catania, Italy*
[5]*Institut für Theoretische Physik, Universität Regensburg, D-93040 Regensburg, Germany*
[6]*Departamento de Química Física, Universidad del País Vasco–Euskal Herriko Unibertsitatea, Apdo. 644, 48080 Bilbao, Spain*
[7]*IKERBASQUE, Basque Foundation for Science, Alameda Urquijo 36, 48011 Bilbao, Spain*
(Received 16 November 2009; revised manuscript received 8 March 2010; published 14 April 2010)

We present a method for measuring the internal state of a superconducting qubit inside an on-chip microwave resonator. We show that one qubit state can be associated with the generation of an increasingly large cavity coherent field, while the other remains associated with the vacuum. By measuring the outgoing resonator field with conventional devices, an efficient single-shot QND-like qubit readout can be achieved, enabling a high-fidelity measurement in the spirit of the electron-shelving technique for trapped ions. We expect that the proposed ideas can be adapted to different superconducting qubit designs and contribute to the further improvement of qubit readout fidelity.

DOI: 10.1103/PhysRevB.81.134514 PACS number(s): 03.65.Yz, 03.65.Wj, 03.67.Lx, 42.50.Lc

Superconducting nanocircuits[1,2] are considered promising candidates for diverse implementations of quantum information tasks.[3] In this context, circuit quantum electrodynamics (QED),[4,5] which studies superconducting qubits[1,6] coupled to on-chip microwave resonators, occupies a central role. To achieve the desired goals, it is important to implement high-fidelity two-qubit gates[7] and efficient schemes to read out the qubit state.[8] To both these ends, trapped-ion systems represent the state-of-the-art for qubit realizations.[9] In particular, electron-shelving qubit readout has produced fidelity benchmarks of approximately 99.99%.[10] These astonishing achievements suggest the potential impact of transferring key ideas from quantum optics to circuit QED. In this paper we show that a single-shot QND-like fast qubit readout can be designed by exploiting the electron-shelving concept in circuit QED.

We first present the physics of electron shelving in trapped ions. In Fig. 1, we show a three-level atom where an unknown qubit state $|\psi\rangle=\alpha|\mathrm{g}\rangle+\beta|\mathrm{e}\rangle$ is encoded in states $|\mathrm{g}\rangle$ and $|\mathrm{e}\rangle$. Via a laser beam, the ground state $|\mathrm{g}\rangle$ is coupled to a third level $|\mathrm{u}\rangle$, which can decay producing a continuous cyclic transition. In this case, the qubit is projected onto state $|\mathrm{g}\rangle$ and many photons are emitted in free space, one at each cycle. In contrast, when the qubit is projected onto state $|\mathrm{e}\rangle$, no photons are emitted. A lens is used to collect the photons more efficiently by improving the solid angle. Although the photodetector has a low efficiency η_{d},[11] the qubit readout fidelity can be very high. Typically, it is estimated through $F=1-e^{-\eta_{\mathrm{d}}N}$, which rapidly approaches unity for $\eta_{\mathrm{d}}N\gg 1$, N being the number of emitted photons.

We present now a method for implementing a single-shot QND-like fast high-fidelity readout of superconducting qubits. It preserves the spirit of electron shelving, but it is suitably adapted to existent microwave technology in circuit QED. We assume that the qubit is prepared in an unknown pure state and that our task is to measure the spin operator σ^z. We consider a three-level superconducting qubit[12,13] inside an on-chip microwave resonator (acting as a cavity), as shown in Fig. 2. The initial qubit state is encoded in the two lower energy levels, $|\psi(0)\rangle=\alpha|\mathrm{g}\rangle+\beta|\mathrm{e}\rangle$. In addition, we consider that the third level is far apart, so that the anharmonic transition frequencies are different: $\omega_{\mathrm{ge}}\neq\omega_{\mathrm{eu}}$. Levels $|\mathrm{e}\rangle$ and $|\mathrm{u}\rangle$ are coupled resonantly to a resonator mode, but there is no dynamics because the resonator is initially empty and level $|\mathrm{u}\rangle$ unpopulated. To start with the readout process, we drive the transition between levels $|\mathrm{e}\rangle$ and $|\mathrm{u}\rangle$ with a coherent resonant field with angular frequency ω_{d} and amplitude μ transversal to the resonator axis.

The system Hamiltonian, after rotating-wave approximation and in the energy eigenbasis, can be written as

$$H=\frac{\hbar\omega_{\mathrm{eu}}}{2}\sigma_{\mathrm{eu}}^{z}+\hbar\omega_{\mathrm{r}}a^{\dagger}a+\hbar g_{\mathrm{eu}}(\sigma_{\mathrm{eu}}^{+}a+\sigma_{\mathrm{eu}}^{-}a^{\dagger})+\hbar\Omega_{\mathrm{eu}}(\sigma_{\mathrm{eu}}^{+}e^{-i\omega_{\mathrm{d}}t}+\sigma_{\mathrm{eu}}^{-}e^{i\omega_{\mathrm{d}}t})+\hbar\lambda(a^{\dagger}e^{-i\omega_{\mathrm{d}}t}+ae^{i\omega_{\mathrm{d}}t}). \quad (1)$$

Here, $\sigma_{\mathrm{eu}}^{z}\equiv|\mathrm{u}\rangle\langle\mathrm{u}|-|\mathrm{e}\rangle\langle\mathrm{e}|$, $\sigma_{\mathrm{eu}}^{+}\equiv|\mathrm{u}\rangle\langle\mathrm{e}|$, $\sigma_{\mathrm{eu}}^{-}\equiv|\mathrm{e}\rangle\langle\mathrm{u}|$, $a(a^{\dagger})$ are the resonator bosonic annihilation (creation) operators, and g_{eu}, Ω_{eu}, and λ are coupling strengths. λ describes the crosstalk between the driving field and the resonator, and its origin typically depends on the specific setup.[14] The qubit readout happens under the resonant condition $\omega_{\mathrm{r}}=\omega_{\mathrm{d}}=\omega_{\mathrm{eu}}$. We assume that the transition $|\mathrm{u}\rangle\rightarrow|\mathrm{e}\rangle$ is sufficiently long lived such that it does not decay during the short detection time. Finally, our model considers enough energy anharmonicity so that the radiative decay rates associated with the transitions $|\mathrm{e}\rangle\rightarrow|\mathrm{g}\rangle$ and $|\mathrm{u}\rangle\rightarrow|\mathrm{g}\rangle$ are not enhanced by the presence of the cavity. Also, these transitions can be reduced exploiting the characteristic selection rules and symmetry breaking properties of superconducting qubits.[13,15,16]

We rewrite the Hamiltonian in a reference frame rotating with the driving field frequency via the transformation $U^{\mathrm{rot}}=\exp[-i\omega_{\mathrm{d}}(a^{\dagger}a+\sigma_{\mathrm{eu}}^{+}\sigma_{\mathrm{eu}}^{-})t]$, obtaining

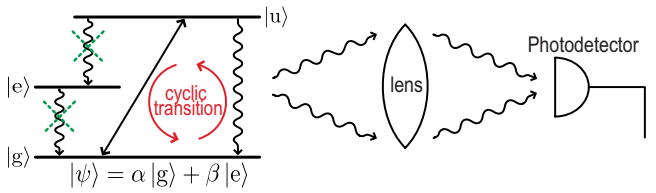

FIG. 1. (Color online) Sketch of electron shelving in trapped ions. The $|g\rangle \leftrightarrow |u\rangle$ transition is driven with a laser beam, performing a cyclic transition and emitting many photons when $|g\rangle$ is projected. No photons are detected when $|e\rangle$ is measured. Undesired transitions are inhibited via selection rules.

$$H^{\mathrm{rot}} = \hbar\Omega_{\mathrm{eu}}\sigma_{\mathrm{eu}}^{x} + \hbar g_{\mathrm{eu}}(\sigma_{\mathrm{eu}}^{+}a + \sigma_{\mathrm{eu}}^{-}a^{\dagger}) + \hbar\lambda(a^{\dagger} + a), \quad (2)$$

with $\sigma_{\mathrm{eu}}^{x} = \sigma_{\mathrm{eu}}^{+} + \sigma_{\mathrm{eu}}^{-}$. We now apply the transformation $U^{I} = \exp[-i\Omega_{\mathrm{eu}}\sigma_{\mathrm{eu}}^{x}t]$ under the strong-driving condition $\Omega_{\mathrm{eu}} \gg g_{\mathrm{eu}}$,[17] and derive the effective Hamiltonian

$$H_{\mathrm{eff}} = \frac{\hbar g_{\mathrm{eu}}}{2}(\sigma_{\mathrm{eu}}^{+} + \sigma_{\mathrm{eu}}^{-})(a + a^{\dagger}) + \hbar\lambda(a^{\dagger} + a). \quad (3)$$

The first part of the Hamiltonian simultaneously realizes Jaynes-Cummings and anti-Jaynes-Cummings resonant interactions. It does not generate Rabi oscillations, but conditional field displacements,[17] while the second term implements a resonant displacement. The initial qubit-field state is $|\psi(0)\rangle = \alpha|g\rangle|0\rangle + \beta(|+\rangle + |-\rangle)|0\rangle/\sqrt{2}$, with $\sigma_{\mathrm{eu}}^{x}|\pm\rangle = \pm|\pm\rangle$. After an interaction time t, the state is

$$|\psi(t)\rangle = \alpha|g\rangle|\bar{\nu}(t)\rangle + \frac{\beta}{\sqrt{2}}[|+\rangle|\bar{\eta}(t) + \bar{\nu}(t)\rangle + |-\rangle|-\bar{\eta}(t) + \bar{\nu}(t)\rangle]. \quad (4)$$

Here, the coherent states $|\pm\bar{\eta}(t) + \bar{\nu}(t)\rangle$, with $\bar{\eta}(t) = -ig_{\mathrm{eu}}t/2$ and $\bar{\nu}(t) = -i\lambda t$, are generated by the displacement operators $\mathcal{D}[\pm\bar{\eta}(t) + \bar{\nu}(t)] = \exp([\pm\bar{\eta}(t) + \bar{\nu}(t)]a^{\dagger} - [\pm\bar{\eta}^{*}(t) + \bar{\nu}^{*}(t)]a)$. In general, we expect the crosstalk to be small, so that $\lambda \ll g_{\mathrm{eu}}/2$ and $\bar{\nu}(t) \ll \bar{\eta}(t)$. When the measurement starts, the applied driving field yields many intracavity photons $\bar{N}_{\mathrm{in}}^{\mathrm{e}}(t) \approx |\bar{\eta}(t)|^2$ with probability $|\alpha|^2$ if the state $|e\rangle$ is projected. If the state $|g\rangle$ is selected, it yields a few photons $\bar{N}_{\mathrm{in}}^{\mathrm{g}}(t) = |\bar{\nu}(t)|^2 \ll |\bar{\eta}(t)|^2$ with probability $|\beta|^2$.

We now add to our model a zero-temperature dissipative reservoir for the cavity field, characterized by a decay rate κ. The corresponding master equation reads

$$\dot{\rho}_{\mathrm{q-f}} = -\frac{i}{\hbar}[H_{\mathrm{eff}}, \rho_{\mathrm{q-f}}] + \mathcal{L}_{\mathrm{f}}\rho_{\mathrm{q-f}}, \quad (5)$$

with $\mathcal{L}_{\mathrm{f}}\rho_{\mathrm{q-f}} \equiv \kappa L[a]\rho_{\mathrm{q-f}}$ such that

$$\mathcal{L}_{\mathrm{f}}\rho_{\mathrm{q-f}} = \frac{\kappa}{2}(2a\rho_{\mathrm{q-f}}a^{\dagger} - a^{\dagger}a\rho_{\mathrm{q-f}} - \rho_{\mathrm{q-f}}a^{\dagger}a) \quad (6)$$

and expansion $\rho_{\mathrm{q-f}}(t) = \Sigma_{j,k=\mathrm{g},-,+}|j\rangle\langle k| \otimes \rho_{\mathrm{f}}^{jk}(t)$. Here, it is possible to find analytical solutions for $\rho_{\mathrm{f}}^{jk}(t) = \langle j|\rho_{\mathrm{q-f}}(t)|k\rangle$ using standard phase-space tools[20] and the method of characteristics to solve the partial differential equations.[21] The solutions read

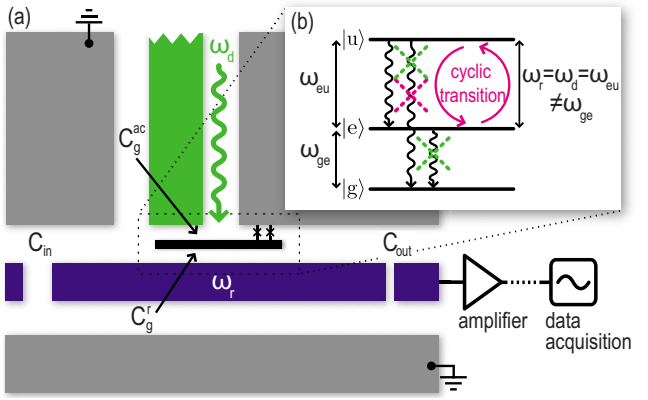

FIG. 2. (Color online) Sketch of the mesoscopic shelving qubit readout. (a) A three-level superconducting qubit is capacitively coupled ($C_{\mathrm{g}}^{\mathrm{r}}$) to a coplanar wave-guide microwave resonator with angular frequency ω_{r} and input and output capacitors C_{in} and C_{out}, respectively. The qubit is also coupled to an orthogonal transmission line via $C_{\mathrm{g}}^{\mathrm{ac}}$. (b) The transition ω_{eu} is resonant to the cavity and is driven with a transversal coherent field. The transition rate $|u\rangle \rightarrow |g\rangle$ may be reduced due to a selection rule.

$$\rho_{\mathrm{f}}^{++}(t) = \frac{|\beta|^2}{2}|\eta(t) + \nu(t)\rangle\langle\eta(t) + \nu(t)|,$$

$$\rho_{\mathrm{f}}^{--}(t) = \frac{|\beta|^2}{2}|-\eta(t) + \nu(t)\rangle\langle-\eta(t) + \nu(t)|,$$

$$\rho_{\mathrm{f}}^{\mathrm{gg}}(t) = |\alpha|^2|\nu(t)\rangle\langle\nu(t)|,$$

$$\rho_{\mathrm{f}}^{+-}(t) = \frac{|\beta|^2}{2}\frac{f_1(t)}{e^{-2|\eta(t)|^2}}|\eta(t) + \nu(t)\rangle\langle-\eta(t) + \nu(t)|,$$

$$\rho_{\mathrm{f}}^{\mathrm{g}+}(t) = \frac{\beta^{*}\alpha}{\sqrt{2}}\frac{f_2(t)}{e^{-|\eta(t)|^2/2}}|\nu(t)\rangle\langle\eta(t) + \nu(t)|,$$

$$\rho_{\mathrm{f}}^{\mathrm{g}-}(t) = \frac{\beta^{*}\alpha}{\sqrt{2}}\frac{f_2(t)}{e^{-|\eta(t)|^2/2}}|\nu(t)\rangle\langle-\eta(t) + \nu(t)|, \quad (7)$$

where

$$f_1(t) = \exp\left(-2\frac{g_{\mathrm{eu}}^2}{\kappa}t + \frac{4g_{\mathrm{eu}}^2}{\kappa^2}[1 - e^{-\kappa t/2}]\right),$$

$$f_2(t) = \exp\left(-\frac{g_{\mathrm{eu}}^2}{2\kappa}t + \frac{g_{\mathrm{eu}}^2}{\kappa^2}[1 - e^{-\kappa t/2}]\right), \quad (8)$$

with $\eta(t) = -ig_{\mathrm{eu}}/\kappa[1 - e^{-\kappa t/2}]$, $\nu(t) = -2i\lambda/\kappa[1 - e^{-\kappa t/2}]$. For a small crosstalk λ, the leakage rate of outgoing photons $N_{\mathrm{out}}^{\mathrm{e}}(t)$ when state $|e\rangle$ is measured can be estimated as

$$N_{\mathrm{out}}^{\mathrm{e}}(t) = \kappa N_{\mathrm{in}}^{\mathrm{e}}(t) = \kappa|\eta(t)|^2 = \frac{g_{\mathrm{eu}}^2}{\kappa}(1 - e^{-\kappa t/2})^2, \quad (9)$$

where $N_{\mathrm{in}}^{\mathrm{e}}(t) = |\eta(t)|^2$ is the intracavity mean photon number. $N_{\mathrm{out}}^{\mathrm{e}}(t)$ grows very fast well below decoherence times. It can

be measured, e.g., by means of a data acquisition card, which follows a phase-preserving or even a more quiet phase-sensitive[18] linear amplifier. We also notice that one can profit from the generated large intracavity field to adapt to other readout techniques.[19]

The physical concepts behind the mesoscopic shelving are general and can be adapted to different qubits and setups. We exemplify here with a possible adaptation to a Cooper-pair box (CPB) coupled to a microwave resonator of angular frequency ω_r. Here, the CPB has a Josephson energy E_J and charging energy $E_C=(2e)^2/2C_{tot}$, where C_{tot} is the total island capacitance. We refer to a system that is essentially the one in Ref. 4, with the addition of a transmission line, orthogonal to the resonator, for driving the qubit (see Fig. 2). Using n, the number operator for excess Cooper pairs on the CPB island, and φ, the phase difference across the Josephson junction, the Hamiltonian can be written as

$$H = E_C(n-n_x)^2 - E_J\cos\varphi + \hbar\omega_r a^\dagger a, \tag{10}$$

where

$$(2e)n_x = C_g^{dc}V_g^{dc} + C_g^{ac}V_g^{ac}(t) + C_g^{r}V_0(a^\dagger + a). \tag{11}$$

Here, C_g^l ($l=\{\mathrm{dc},\mathrm{ac},\mathrm{r}\}$) are effective gate capacitances, V_g^{dc} is the gate voltage that defines the working point (we choose the so-called "sweet spot" $C_g^{dc}V_g^{dc}/2e=1/2$), V_g^{ac} is the voltage of the orthogonal driving field, a ($a^\dagger$) refers to the cavity field, and V_0 is the resonator zero-point voltage. Note that the CPB is coupled to the resonator and the ac drive via the charge number operator. The classical gate charge $C_g^{ac}V_g^{ac}$ and the quantum gate charge $C_g^{r}V_0$ represent small deviations from the sweet spot.

We can rewrite H in a basis of CPB eigenstates restricted to the first three energy levels, the ground state $|\mathrm{g}\rangle$ and the first and second excited states, $|\mathrm{e}\rangle$ and $|\mathrm{u}\rangle$, respectively. This leads to an effective Hamiltonian for the driven qubit-resonator system,

$$\mathcal{H} = \mathcal{H}_0 + \mathcal{H}_{int} + \mathcal{H}_d,$$

$$\mathcal{H}_0 = \sum_{j=\mathrm{g,e,u}} E_j|j\rangle\langle j| + \hbar\omega_r a^\dagger a,$$

$$\mathcal{H}_{int} = \hbar(g_{ge}|\mathrm{e}\rangle\langle\mathrm{g}| + g_{eu}|\mathrm{u}\rangle\langle\mathrm{e}|)(a^\dagger + a) + \mathrm{H.c.},$$

$$\mathcal{H}_d = (\cos\omega_d t)\sum_{j<k=\mathrm{g,e,u}} (\hbar\Omega_{jk}|j\rangle\langle k| + \mathrm{H.c.}). \tag{12}$$

The coupling strengths $g_{jk}\equiv(E_C/\hbar e)n_{jk}C_g^{r}V_0$ and $\Omega_{jk}\equiv(E_C/\hbar e)n_{jk}C_g^{ac}V_g^{ac}(t)$ are proportional to the matrix elements $n_{jk}=\langle k|n|j\rangle$. In order to obtain the time evolution of the complete system, including the relaxation and dephasing of qubit transitions, we numerically solve the master equation for the qubit-resonator density matrix $\rho(t)$

$$\dot\rho = -\frac{i}{\hbar}[\mathcal{H},\rho] + \mathcal{L}_f\rho + \mathcal{L}_q\rho, \tag{13}$$

where, using the functional L defined in Eq. (5), we have

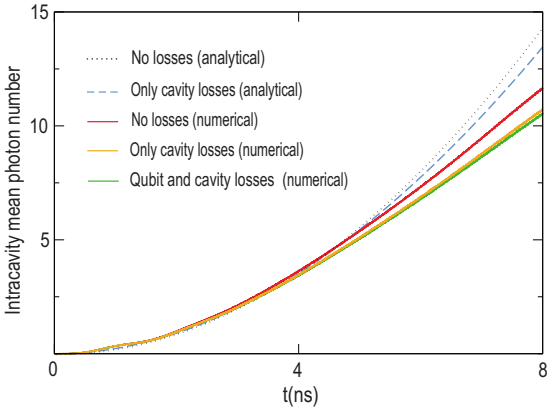

FIG. 3. (Color online) Intracavity mean photon number for the mesoscopic shelving readout of a CPB in the charge-phase regime with conservative parameter set: $E_C/\hbar=E_J/\hbar=2\pi\times10$ GHz, $g_{eu}=\Omega_{eu}/5=2\pi\times150$ MHz, $\kappa=2\pi\times1.6$ MHz, $\gamma_{eu}=10\gamma_{ge}=2$ MHz, $\gamma_{gu}=0$, and $\gamma_\varphi=2$ MHz. The dotted and dashed curves correspond to the analytical results and the solid lines to the numerical results (all curves appear and are listed from up to bottom). Note that, in the absence of losses, there is still a difference between the analytical and the numerical results. This is due to the off-resonant couplings and multilevel character of the realistic model.

$$\mathcal{L}_q\rho = \sum_{j<k}\gamma_{jk}L[|k\rangle\langle j|]\rho + \sum_j\frac{\gamma_\varphi}{2}L[|j\rangle\langle j|]\rho. \tag{14}$$

Here, κ is the decay rate of the resonator, γ_{jk} ($j,k=\{\mathrm{g,e,u}\}$) are the relaxation rates for the transitions $|\mathrm{e}\rangle\rightarrow|\mathrm{u}\rangle$ and $|\mathrm{u}\rangle\rightarrow|\mathrm{g}\rangle$, and γ_φ is the dephasing rate, which we take to be equal for all coherences. In the numerical solution of Eq. (13), we truncate the resonator Hilbert space to 25 photon number states due to technical limitations. In addition, we make sure that the population of the fourth qubit eigenstate is negligible. Clearly, the condition $\gamma_{eu}+\gamma_{gu}\ll g_{eu}$ is crucial for our method to be efficient. Therefore, a qubit layout with suppressed γ_{gu} is preferred for the shelving readout.

The results for the intracavity mean photon number with a conservative set of parameters, in the analytical and numerical cases, are shown in Fig. 3. We see that, although the full dynamics in Eq. (13) is considerably more complex than the one in Eq. (5), the simple analytical model captures the essence of the system dynamics. The main influence of a realistic description is a small reduction in the intracavity mean photon number. We observe that, given the short interaction times displayed in Fig. 3, the resonator decay rate κ alone has a small effect in the cavity population, while the finite lifetime of states $|\mathrm{e}\rangle$ and $|\mathrm{u}\rangle$ is slightly more important. In this manner, we feel comfortable to extrapolate the analytical results for the cavity population including cavity losses for short measurement times to make further estimations. Note that in the simulations of the full system with initial state $|\mathrm{g}\rangle$, we observe an intracavity mean photon number that does not exceed 5% of the corresponding photon number for the initial state $|\mathrm{e}\rangle$ (where we use a sizeable crosstalk of $\lambda=2\pi\times10$ MHz). Thus, we expect the parasitic cavity population in an experiment to remain well within the noise level.

Clearly, the parameter which determines the speed of the mesoscopic shelving readout is the Jaynes-Cummings coupling g_{eu} that drives the shelving transition, and one still has to respect the condition of strong driving $\Omega_{eu} \gg g_{eu}$. On the other hand, the cavity decay time $1/\kappa$ must be much larger than the measuring time in order to facilitate intracavity photon accumulation.

Our example refers to the "quantronium regime" of a CPB ($E_J = E_C$). Simulations in the transmon regime ($E_J/E_C = 8$) reveal that the qualitative behavior is still the one shown in Fig. 3, however, the deviations of the full simulation compared to the analytical model are larger (i.e., the mean cavity photon number grows more slowly compared to $(g_{eu}t)^2/4$ than for $E_J/E_C = 1$). This shows that a large anharmonicity of the qubit circuit increases the efficiency of the mesoscopic shelving readout. Circuits that exhibit a selection rule for transitions between states $|u\rangle$ and $|g\rangle$ (e.g., the CPB and the transmon) may have an advantage with respect to, e.g., the phase qubit or the flux qubit (which, however, is significant only if the measuring time is comparable to the relaxation rate $|u\rangle \rightarrow |g\rangle$).

The signal-to-noise ratio (SNR) after a measurement time τ_m is the ratio between the accumulated number of outgoing photons and the accumulated noise.[4] The latter is dominated by the amplifier noise, $n_{amp} = k_B T_n/\hbar\omega_r \simeq 25$, where T_n is its noise temperature. Note that, if the initial state of the qubit is $|g\rangle$, the simulation yields a final cavity photon number that is negligible compared to the typical noise level. In this manner,

$$\mathrm{SNR}(\tau_m) = \frac{\int_0^{\tau_m} \kappa N_{in}^e(t)dt}{n_{amp} B \tau_m}, \tag{15}$$

where $B \equiv \max\{\kappa, \gamma_{jk}\}$ is the measurement bandwidth. We now estimate the SNR for three relevant consecutive times. First, we use the maximum simulated time $\tau_m^{sim} \simeq 8$ ns, corresponding to ten intracavity photons (cf. Fig. 3). We obtain a SNR $\simeq 0.2$. Considering that our simulations include all relevant system details without any approximation,[22] this is a remarkable result for such an extremely short measurement time. Using our analytical results including resonator dissipation, see Eq. (9), we estimate that a critical measurement time $\tau_m^{crit} \simeq 19$ ns is necessary to reach the condition SNR ~ 1. This is the minimum time required for a single-shot measurement of the qubit state $|e\rangle$. Finally, to achieve high-fidelity qubit readout, we choose the measurement time $\tau_m^{hf} \simeq 50$ ns which corresponds to SNR $\simeq 6.2$ and fidelity $F \simeq 99\%$ according to the infinite-lifetime model in Ref. 23 (the infinite-lifetime model appears appropriate here due to the smallness of the measuring time compared to the relaxation time: $\tau_m^{hf} \ll 1/\gamma_{eu}$).

Consequently, we expect a single-shot measurement of the qubit state $|e\rangle$ with fidelities close to 1. The proposed mesoscopic shelving qubit readout is of a QND-like character, in the same sense as electron shelving,[9] due to the continuous cavity field amplification in each measurement event. In addition, τ_m^{hf} is at least one order of magnitude shorter than typical measurement times employed in the state-of-the-art experiments based on dispersive readouts.

In summary, we have presented a novel qubit readout scheme based on a mesoscopic shelving technique, allowing a fast high-fidelity single-shot QND-like measurement of superconducting qubits in circuit QED.

We acknowledge discussions with P. Bertet, M. Hofheinz, A. Wallraff, J. M. Martinis, R. Schoelkopf, R. Bianchetti, and F. Deppe. This work is funded by Deutsche Forschungsgemeinschaft through SFB 631, Heisenberg Programme, German Academic Exchange Service, and German Excellence Initiative Nanosystems Initiative Munich (NIM). E.S. acknowledges support from UPV-EHU Grant No. GIU07/40, Ministerio de Ciencia e Innovación Grant No. FIS2009-12773-C02-01, EuroSQIP and SOLID European projects.

*Present address: Max-Planck-Institut für Quantenoptik, Hans-Kopfermann-Str. 1, D-85748 Garching, Germany.

†Present address: Department of Physics, University of California, Santa Barbara, California 93106, USA.

[1] Y. Makhlin, G. Schön, and A. Shnirman, Rev. Mod. Phys. **73**, 357 (2001).

[2] J. Q. You and F. Nori, Phys. Today **58**, 42 (2005); J. Clarke and F. K. Wilhelm, Nature (London) **453**, 1031 (2008).

[3] D. Bouwmeester, A. Ekert, and A. Zeilinger, *The Physics of Quantum Information* (Springer Verlag, Berlin, 2008).

[4] A. Blais, R.-S. Huang, A. Wallraff, S. M. Girvin, and R. J. Schoelkopf, Phys. Rev. A **69**, 062320 (2004).

[5] I. Chiorescu, P. Bertet, K. Semba, Y. Nakamura, C. J. P. M. Harmans, and J. E. Mooij, Nature (London) **431**, 159 (2004); A. Wallraff, D. I. Schuster, A. Blais, L. Frunzio, R.-S. Huang, J. Majer, S. Kumar, S. M. Girvin, and R. J. Schoelkopf, *ibid.* **431**, 162 (2004).

[6] Y. Nakamura, Yu. Pashkin, and J. S. Tsai, Nature (London) **398**, 786 (1999).

[7] T. Yamamoto, Yu. A. Pashkin, O. Astafiev, Y. Nakamura, and J. S. Tsai, Nature (London) **425**, 941 (2003); R. McDermott *et al.*, Science **307**, 1299 (2005); J. H. Plantenberg, P. C. de Groot, C. J. P. M. Harmans, and J. E. Mooij, Nature (London) **447**, 836 (2007).

[8] I. Siddiqi, R. Vijay, F. Pierre, C. M. Wilson, M. Metcalfe, C. Rigetti, L. Frunzio, and M. H. Devoret, Phys. Rev. Lett. **93**, 207002 (2004); A. Wallraff, D. I. Schuster, A. Blais, L. Frunzio, J. Majer, M. H. Devoret, S. M. Girvin, and R. J. Schoelkopf, *ibid.* **95**, 060501 (2005); M. Steffen, M. Ansmann, R. McDermott, N. Katz, R. C. Bialczak, E. Lucero, M. Neeley, E. M. Weig, A. N. Cleland, and J. M. Martinis, *ibid.* **97**, 050502 (2006); A. Lupascu, S. Saito, T. Picot, P. C. de Groot, C. J. P. M. Harmans, and J. E. Mooij, Nat. Phys. **3**, 119 (2007).

[9] D. Leibfried, R. Blatt, C. Monroe, and D. Wineland, Rev. Mod. Phys. **75**, 281 (2003).

[10] D. B. Hume, T. Rosenband, and D. J. Wineland, Phys. Rev. Lett.

99, 120502 (2007); A. H. Myerson, D. J. Szwer, S. C. Webster, D. T. C. Allcock, M. J. Curtis, G. Imreh, J. A. Sherman, D. N. Stacey, A. M. Steane, and D. M. Lucas, *ibid.* **100**, 200502 (2008).

[11] Microwave photodetectors are currently unavailable. However, see G. Romero, J. J. García-Ripoll, and E. Solano, Phys. Rev. Lett. **102**, 173602 (2009); Phys. Scr. **T137**, 014004 (2009).

[12] J. Siewert and T. Brandes, Adv. Solid State Phys. **44**, 181 (2004); E. Paspalakis and N. J. Kylstra, J. Mod. Opt. **51**, 1679 (2004); J. Siewert, T. Brandes, and G. Falci, Opt. Commun. **264**, 435 (2006).

[13] Yu-Xi Liu, J. Q. You, L. F. Wei, C. P. Sun, and F. Nori, Phys. Rev. Lett. **95**, 087001 (2005).

[14] M. Mariantoni, F. Deppe, A. Marx, R. Gross, F. K. Wilhelm, and E. Solano, Phys. Rev. B **78**, 104508 (2008).

[15] F. Deppe, M. Mariantoni, E. P. Menzel, A. Marx, S. Saito, K. Kakuyanagi, H. Tanaka, T. Meno, K. Semba, H. Takayanagi, E. Solano, and R. Gross, Nat. Phys. **4**, 686 (2008).

[16] F. Helmer, M. Mariantoni, A. G. Fowler, J. von Delft, E. Solano, and F. Marquardt, Europhys. Lett. **85**, 50007 (2009).

[17] E. Solano, G. S. Agarwal, and H. Walther, Phys. Rev. Lett. **90**, 027903 (2003).

[18] M. A. Castellanos-Beltran, K. D. Irwin, G. C. Hilton, L. R. Vale, and K. W. Lehnert, Nat. Phys. **4**, 929 (2008); T. Yamamoto, K. Inomata, M. Watanabe, K. Matsuba, T. Miyazaki, W. D. Oliver, Y. Nakamura, and J. S. Tsai, Appl. Phys. Lett. **93**, 042510 (2008).

[19] M. Hofheinz, E. M. Weig, M. Ansmann, R. C. Bialczak, E. Lucero, M. Neeley, A. D. O'Connell, H. Wang, J. M. Martinis, and A. N. Cleland, Nature (London) **454**, 310 (2008).

[20] P. Lougovski, F. Casagrande, A. Lulli, and E. Solano, Phys. Rev. A **76**, 033802 (2007).

[21] S. M. Barnett and P. M. Radmore, *Methods in Theoretical Quantum Optics* (Oxford University Press, New York, 1997).

[22] M. Boissonneault, J. M. Gambetta, and A. Blais, Phys. Rev. A **77**, 060305(R) (2008).

[23] J. M. Gambetta, W. A. Braff, A. Wallraff, S. M. Girvin, and R. J. Schoelkopf, Phys. Rev. A **76**, 012325 (2007).